Scientific paper

Filming Atomic Motions in Liquids

Savo Bratos,[1] Guilhem Gallot,[2] Jean-Claude Leicknam,[1] Stanislas Pommeret,[3] Rodolphe Vuilleumier[4] and Michael Wulff[5]

[1] *Laboratoire de Physique Théorique de la Matière Condensée, Université Pierre et Marie Curie, Case courrier 121, 4, Place Jussieu, 75252 Paris Cedex, France*

[2] *Laboratoire d'Optique et Biosciences, Ecole Polytechnique, Route de Saclay, 91128 Palaiseau Cedex, France*

[3] *CEA/Saclay, DSM/IRAMIS, SIS2M UMR 3299, 91191 Gif-sur-Yvette Cedex, France.*

[4] *Ecole Normale Supérieure, Dpt de Chimie, 24, rue Lhomond, 75231 Paris Cedex, France*

[5] *European Synchrotron Radiation Facility, BP 220, 38043 Grenoble Cedex, France*

* *Corresponding author: E-mail: bratos@lptl.jussieu.fr*

Received: 21-04-2011

Dedicated to Professor Dušan Hadži on the occasion of his 90th birthday

Abstract

Basic techniques in ultrafast time-resolved optical spectroscopy and x-ray diffraction are described for a broad scientific community. Basic experimental setups are presented, and theories for the interpretation of experimental data are briefly described. The power of these ultrafast techniques is shown with a few selected examples. It is shown in particular how they permit to film atomic motions during a chemical reaction. The strong and weak points of the two complementary techniques are discussed in some detail. A number of basic references are included to help interested readers. Future developments of ultrafast techniques are conjectured at the end of the paper.

Keywords: Liquids, visualizing molecular motions, chemical reactions, pump-probe spectroscopy, time-resolved X-ray diffraction

1. Introduction

It has always been a dream of physicists and chemists to follow atomic motions during a chemical reaction in real time. Unfortunately, atomic dimensions are small and atoms evolve on ultrafast time scales, typically between 10 fs and 100 ps. This is why this dream remained a dream over two centuries following Lavoisier's foundation of chemistry. The situation is very different today due to new experimental developments. Two methods are particularly important for probing atomic motions in reactions. The first is ultrafast optical spectroscopy, which captures ultrafast energy changes due to molecular rearrangements; for excellent text-books see e.g.[1–3] This method is very efficient but, as the wavelength of the visible light is large compared to molecular dimensions, extra information is required to deduce molecular geometry from spectral data. This difficulty is absent in the second major technique of this field, time-resolved x-ray diffraction and absorption; unfortunately, only a limited number of review papers cover this field as yet.[4–6] In this method molecular structures are probed directly due to the short wavelength of x-rays. However, large scale synchrotron sources, or free electron lasers based on linear accelerators are required for these experiments. These "non-human" characteristics of such large scale facilities are sometimes considered a drawback of this technique.

The purpose of this paper is to present these methods briefly to a broad scientific community. Time-resolved electron diffraction, more adapted to the study of diluted systems, will not be discussed. Experimental techniques are briefly described, and the basic elements of the theory are sketchily presented in what follows. We decided to treat optical and x-ray techniques separately in two distinct chapters. Their power is illustrated with a few selected examples, taken from the work of our research groups. Although written for a broad community, this pa-

per describes the current state-of-the-art. It is dedicated to Prof. S. Hadzi who directed the first steps in science of one of us (S.B).

2. Nonlinear Optical Spectroscopy

2. 1. Generalities

A large number of time-resolved optical techniques have been developed. In so-called four-wave mixing techniques, the system is submitted to three laser fields with wave vectors $\mathbf{k}_1$, $\mathbf{k}_2$, $\mathbf{k}_3$ and frequencies ω_1, ω_2, ω_3. The fourth field is that of the emerging coherent signal having the wave vector $\mathbf{k}_s$ and the frequency ω_s [1]:

$$\mathbf{k}_s = \pm\mathbf{k}_1 \pm \mathbf{k}_2 \pm\mathbf{k}_3 \; \omega_s = \pm\omega_1 \pm\omega_2 \pm\omega_3$$

Various variants of nonlinear optical spectroscopy differ in the choice of incoming $\mathbf{k_i}$'s and ω_i's. The most familiar examples are pump-probe spectroscopy where $\mathbf{k}_1 = \mathbf{k}_2$ and $\mathbf{k}_3 = \mathbf{k}_s$, coherent antistokes Raman scattering (or CARS) where $\mathbf{k}_1 = \mathbf{k}_3$ and $\mathbf{k}_s = 2\mathbf{k}_1 - \mathbf{k}_2$, or 3-pulse photon echo where $\mathbf{k}_s = \mathbf{k}_3 + \mathbf{k}_2 - \mathbf{k}_1$. The signal field is in the direction $\mathbf{k}_s$; this direction is generally different from that of the incoming wave vectors $\mathbf{k}_i$. Spectral data can often be interpreted in terms of a grating formed by two beams, the third beam undergoing Bragg diffraction from this grating. All these methods have their advantages and disadvantages, and may be chosen according to the purpose of the research project.

Nonlinear optical techniques can be divided into resonant and off-resonant techniques. In the case of a resonant technique, the incident field frequency, or combination of them, is equal to one of characteristic frequencies of the matter. The pump-probe spectroscopy is an example of such techniques. They probe the eigenstates of the system and their dynamical behavior directly. They are also sensitive to relaxation processes such as spontaneous emission. In an off-resonant technique, the incident field frequency is far detuned from the natural frequencies of the system under consideration. Time-resolved Raman scattering is a typical technique of this class. Off-resonant techniques permit to avoid absorptive losses and other competing processes. Resonant and off-resonant techniques are both of common use.

2. 2. Pump-probe Spectroscopy

This technique is the simplest nonlinear optical technique; it will be discussed in the rest of this Section. The basic set-up is as follows (Fig. 1). A powerful laser **L** generates pico- or sub picosecond optical pulses. Each pulse is split by a beam splitter **B** into two pulses, an intense pump pulse $\mathbf{P_1}$ and a weak probe pulse $\mathbf{P_2}$. Their frequencies ω_1, ω_2 are derived from the incident laser frequency ω_L by using suitable optical devices **C** called wave-length tuners. The time delay τ between them is controlled by another device **V** which elongates the optical path at will; it may be considered as a sort of stroboscopic device. The two pulses meet at the sample cell **S** where they mix and interact with matter. Prepared in this way the system is unstable and relaxes back to the equilibrium. This return is monitored measuring the probe absorption for different probe frequencies ω_2 and for different time delays τ.

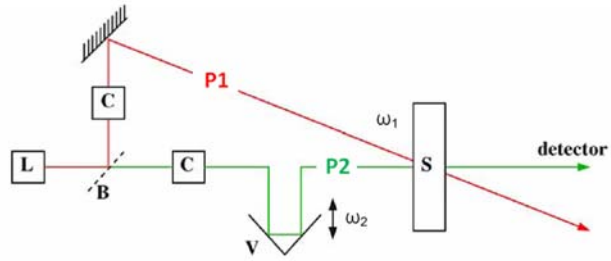

Fig. 1. Schematic representation of an infrared pump-probe set-up.

The measured signal $\Delta S(\omega_1, \omega_2, \tau)$ is defined as time integrated probe absorption $S(\omega_1, \omega_2, \tau)$ in presence of the pump, minus probe absorption $S_0(\omega_2)$ in absence of the pump. This signal may be negative or positive, according to whether $S < S_0$ or $S > S_0$; these two processes are called bleaching and induced absorption, respectively. Experimental data may be presented in one of the following two ways. The signal $\Delta S(\omega_1, \omega_2, \tau)$ may be plotted for a fixed pump frequency ω_1 and a given time delay τ, as a function of the probe frequency ω_2. This is what is called a frequency-resolved spectrum. Alternatively, it can also be recorded for fixed pump and probe frequencies ω_1, ω_2 as a function of the time delay τ. This forms a time-resolved spectrum. Both of them are of current use.

2. 3. Theoretical Considerations

The theory of time-resolved optical spectroscopy is based on the observation that a laser shot brings a system distinctly out of thermal equilibrium. The Kubo linear response theory is no longer valid, and methods from statistical mechanics of nonlinear optical processes must be employed. Let then H_0 denote the quantum-mechanical Hamiltonian of the liquid sample in absence of perturbation. In its presence, the perturbation Hamiltonian can often be written $H_1(t) = -\mathbf{M}.\mathbf{E}(t)$, where $\mathbf{E}(t)$ is the laser generated electric field and **M** the dipole moment of the system. The complete Hamiltonian is then $H = H_0 + H_1$. For samples with a large number of molecules, a statistical description must be adopted. The density matrix $\rho(t)$ permits to do it, and it obeys von Neumann's equation:

$$\partial\rho/\partial t = -(i/\hbar)[H, \rho]$$

The problem thus reduces to that of solving this equation in conditions imposed by the experiment. This is usually done using one or another sort of higher-order perturbation theory; non-perturbative techniques are only rarely employed. Once $\rho(t)$ is known, the average value of any operator O of interest is given by the general formula $\langle O(t) \rangle = Tr [O \rho(t)]$.

This general procedure has been applied successfully to different sorts of non-linear spectroscopy.[2] The electromagnetic fields may be assumed Maxwellian whenever the photon flux is large, e.g. in pump-probe spectroscopy; and quantum-field theory is required whenever they are weak, e.g. in time resolved fluorescence. In principle, the molecular system is supposed to be controlled by quantum mechanics. The resulting theory is characterized by the presence of third-, fourth-, and higher-order time correlation functions. Four-time correlation functions are required for example in pump-probe spectroscopy, whereas six-order correlation functions describe photon echoes experiments. Note that only two-time correlation functions enter into "normal" spectroscopy. If the temperature is high enough, translational and rotational degrees of freedom may be assumed to be classical; they can then be treated by classical molecular dynamics simulations. These remarks also apply to pump-probe spectroscopy, where the operator O is equal to the interaction energy of the probe field with the dipole moment of the system. It is worth noting that the resulting signal $\Delta S(\omega_1, \omega_2, \tau)$ is exact to the third-order in the perturbation.[7]

2. 4. Visualizing OH…O Motions in Liquid Water

A great number of beautiful experiments have been realized using nonlinear spectroscopic techniques, following the pioneering work of A. Zewail, Nobel Prize laureate in 1999. We decided to discuss time-resolved spectroscopic studies of water, the most important liquid on the surface of the earth. More specifically, we shall show how optical techniques can be used to film atomic motions of the OH…O hydrogen bond in liquid water.[8] For practical reasons diluted solutions of HDO in D_2O rather than pure water H_2O were used. Details are as follows.

This water study is an infrared pump-probe experiment. It is based on a widely known empirical relation due to Novak, linking the OH bond vibrational frequency and the OH...O bond length.[9] The stronger the hydrogen bond, the softer the OH link and the lower is its OH frequency ω_0 (Fig. 2a). In our non-linear experiment, an ultrafast pump pulse of frequency ω_1 is used to excite OH vibrations; this excitation results in selecting OH...O bonds of a given length r_1. Let first ω_1 be larger than ω_0, the mean OH frequency of HDO in D_2O (Fig.2b). The laser selected OH…O bonds, the initial length r_1 of which is larger than their equilibrium length r_0, contract with time, and a low frequency shift of the OH band from ω_1 to ω_0 may be anticipated. The opposite behavior is expected if ω_1 is smaller than ω_0 (Fig. 2c). The OH…O bond, initially too short, expands on relaxing and a high frequency shift of the OH band is expected. No band shift should exist if $\omega_1 = \omega_0$. Conversely, knowing the peak frequency $\omega(\tau)$ of the signal measured when the pump-probe time delay is τ, and using the above mentioned empirical relation between OH frequency and OH...O bond length, permits the determination of this distance as a function of τ. These are theoretical predictions.

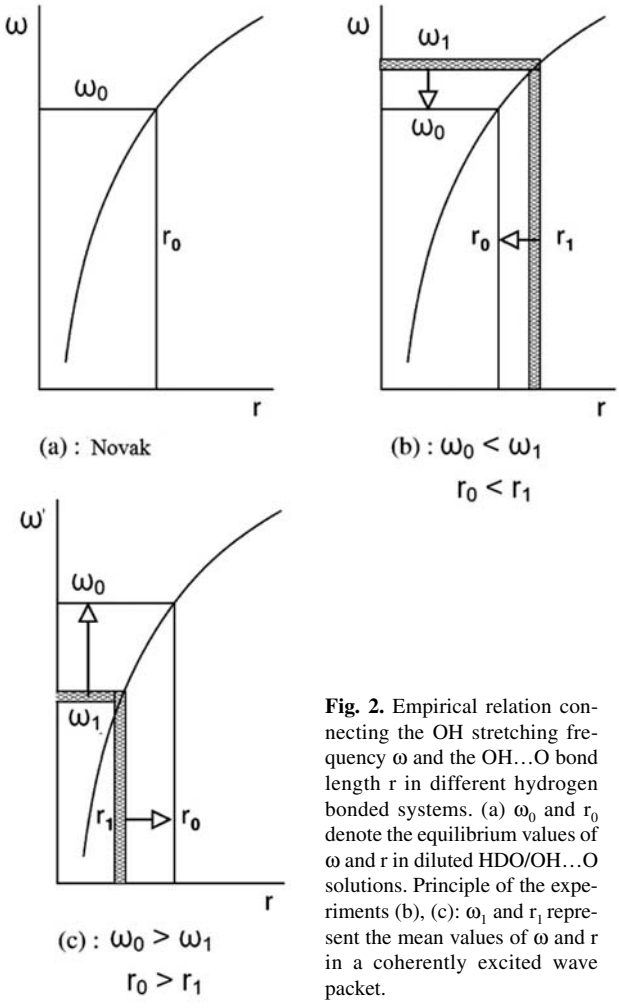

Fig. 2. Empirical relation connecting the OH stretching frequency ω and the OH…O bond length r in different hydrogen bonded systems. (a) ω_0 and r_0 denote the equilibrium values of ω and r in diluted HDO/OH…O solutions. Principle of the experiments (b), (c): ω_1 and r_1 represent the mean values of ω and r in a coherently excited wave packet.

These predictions are completely confirmed by the experiments. Molecular OH…O dynamics were monitored at ω_1 = 3510, 3420 and 3340 cm^{-1} with a time resolution of 150 fs (Fig. 3). If the excitation is at 3510 cm^{-1}, the length of the pump selected hydrogen bonds is r_1 = 2.99 Å, longer than r_0 = 2.86 Å. Fig. 3a thus illustrates the contraction of the initially elongated hydrogen bonds. The excitation is at 3420 cm^{-1} in Fig. 3b and r_1 = 2.86 Å. As $r_1 = r_0$, thermal equilibrium is not destroyed by the pump and there is no variation of r_1. Finally, if the excitation is at 3340 cm^{-1}, the length of selected hydrogen bonds is r_1 =

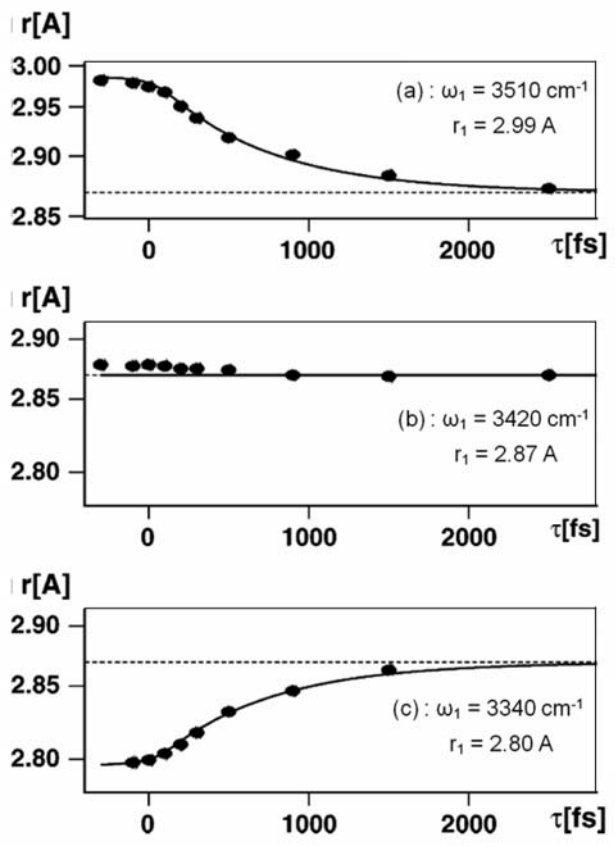

Fig. 3. Real time filming OH…O stretching motions: The length r (τ) of the OH…O bond is expressed as a function of time τ. (a) corresponds to excitation at 3510 cm^{-1}, (b) to 3420 cm^{-1} and (c) to 3340 cm^{-1}. The initial OH…O bond length is 2.99 Å in (a), 2.86 Å in (b) and 2.80 Å in (c). The points represent experimental data.

2.80 Å, shorter than r_0 = 2.86 Å. Fig. 3c shows the extension of the initially compressed hydrogen bonds. Our pump-probe experiment thus permits to film atomic displacements in hydrogen bonds in real time.

This section can be concluded recalling that it is intrinsically difficult to pass from optical spectra to molecular geometry. Extra information is needed to surmount this obstacle. The above analysis is based on the empirical Novak relation connecting the OH frequency to the OH...O hydrogen bond length. This relation has been tested extensively in classical spectroscopy, where the systems remain close to thermal equilibrium. It is still valid in laser excited systems that are far from thermal equilibrium? Is it fine enough to follow their temporal evolution? To answer these questions, we reexamined the problem theoretically.[10] The laser generated non-equilibrium was treated in the frame of statistical mechanics of non-equilibrium systems.[2] Quantum mechanics was employed to study vibrational degrees of freedom of dissolved HDO molecules, whereas rotational-translational degrees of freedom of the HDO/D_2O solution were examined by classical molecular dynamics simulation. It results from this analysis that the Novak relationship remains *valid down to times of the order of 100 fs* (Fig. 4). It can be used only with great precaution at shorter times, where collisions between water molecules dominate. For further reading about ultrafast spectroscopy of water.[11–18]

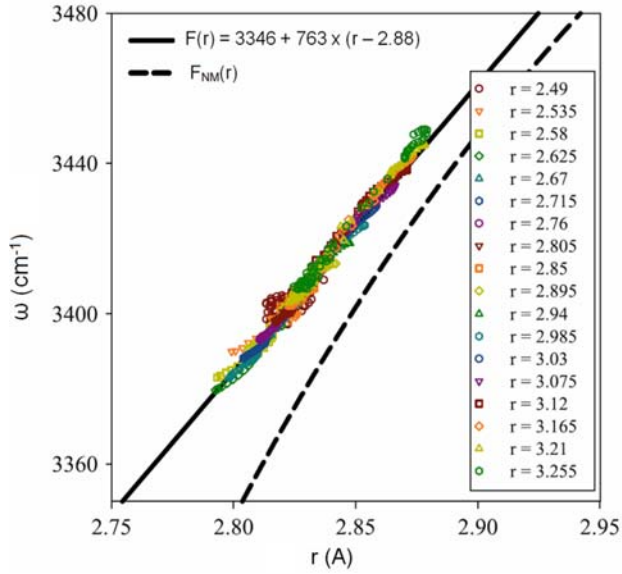

Fig. 4. Distribution of the computer calculated OH frequencies ω at different OH…O distances r. Each point corresponds to a given value of time elapsed after the initial laser shot, and to the corresponding oxygen-oxygen distance. The calculations were realized considering 18 initial OH…O configurations indicated by color, and 100 times comprised between 150 and 3000 fs. The calculated points strongly concentrate around a straight line. The dashed line is a plot of the Novak relation.

3. Time-Resolved X-Ray Diffraction

3. 1. Generalities

Two major sorts of time-resolved x-ray experiment exist.[4–6] In both of them the system is brought out of thermal equilibrium by an ultrafast laser pulse. Laser induced change of the system is then observed either by diffraction or by absorption of x-rays. These two approaches are very different from each other. The first of them permits to monitor global as well as local changes of the system, whereas the second is better adapted to follow local changes. Absorption techniques comprise methods like extended x-ray absorption fine structure (EXAFS) and near-edge structure (XANES). These diffraction and absorption methods permit to visualize atomic motions in liquids. Note however that they do not permit to follow stochastic motions of each atom individually. But they permit to follow them in terms of time dependent atom-atom distribution functions.

Technological constraints are particularly heavy in x-ray physics, much more so than in optical spectroscopy. If a static x-ray experiment can be realized with a small x-ray generator in a room, synchrotrons with dimensions of the order of hundreds of meters are needed to attain intense 100 ps x-ray pulses (Fig. 5). And 2 km long linear accelerators in free electron laser – or XFEL – sources are required to generate 10–100 fs pulses. One such source is actually operating in Stanford (USA), and several are under construction around the world. It should be emphasized that not only technological, but also theoretical efforts are needed to study femtosecond phenomena.

Fig. 5. Photograph of the European Synchrotron Radiation Facility (ESRF) in Grenoble. The synchrotron ring is seen in the center of the figure.

3. 2. Pump-probe X-ray Diffraction

This is the simplest time-resolved x-ray diffraction experiment, the only one illustrated in this Section (Fig. 6). The liquid system under consideration is pumped by a laser, which promotes a fraction of molecules into one or several excited quantum states. The laser deposited energy diffuses into the system in one or several steps, generating several sorts of events. If the excitation is in the optical spectral range, chemical reaction may be triggered and in addition the sample is heated. If it is in infrared, only heating is generally present. The return of the system to thermal equilibrium is probed using a series of time-delayed x-ray pulses. The resulting diffraction pattern consists of circular rings, centered on the forward beam. The collection of x-ray patterns obtained in this way can be transformed into a collection of molecular photographs; this step is accomplished by theory as discussed below. A time-resolved x-ray experiment permits to film atomic motions in space and time.

Several sorts of x-ray signals appear in this sort of experiments. The measured quantity is the difference signal $\Delta S(q,\tau) = S(q,\tau) - S_{eq}(q)$, defined as the time-integrated x-ray energy flux $S(q,\tau)$ scattered in a given solid angle in presence of the pump, minus the time-integrated x-ray energy flux $S_{eq}(q)$ scattered in the same solid angle in the absence of the pump. It depends on two variables: the scattering wave vector $q = |\mathbf{q_I} - \mathbf{q_S}|$ where $\mathbf{q_I}$ and $\mathbf{q_S}$ are wave vectors of the incident and scattered x-ray radiation,

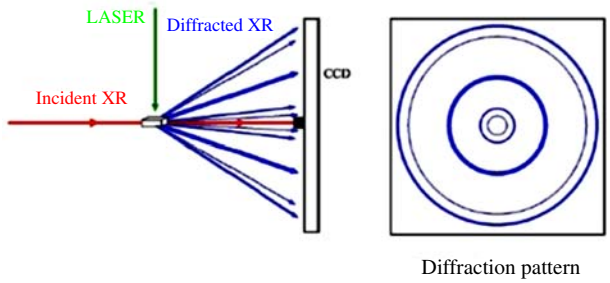

Fig. 6. Schematic representation of the experimental set-up (left), and of the observed x-ray diffraction pattern (right). In practice, the x-ray and laser beams are not perpendicular to each other, and the cell containing the liquid is replaced by a jet of liquid.

respectively, and the time delay τ between pump and probe. The Fourier sine transform $\Delta S[r,\tau]$ of $\Delta S(q,\tau)$ is also very important. Expressible in terms of atom-atom distribution functions $g_{\mu\nu}(r,t)$, it provides information about changes in molecular geometry during a chemical reaction. Here the variable r designates the distance between atoms μ and ν at time t. This Fourier transformed signal is the central object of this sort of research.

3. 3. Theoretical Considerations

The first theoretical attempts to study pump-probe x-ray diffraction were entirely empirical. More precise theoretical work appeared only in the late 1990s from Wilson and co-workers.[19] However, this work remained preliminary. A realistic approach is statistical again, and uses the density matrix approach. Somewhat surprisingly, theories for time-resolved spectroscopy and time-resolved diffraction are much more similar than are the corresponding experimental techniques.

A statistical theory of this sort has been published several years ago.[20] It rests on the following elements: (1) Incident electric and magnetic fields are Maxwellian. They represent plane waves with a carrier frequency ω_x, but their amplitudes $E_{x0}(t)$ and $H_{x0}(t)$ vary slowly with time. The last statement also applies to the electronic density $n(\mathbf{r},t)$ of the system, and to its Fourier transform $f(\mathbf{q},t)$; this latter quantity is generally called form factor. (2) The molecular system is described by standard quantum mechanics. (3) The frequencies of the pumping optical and probing x-ray field differ from each other by a factor of the order of 10^3. Pumping and probing processes can thus be treated separately, one after the other. Consi-

dering these points the pump-probe x ray diffraction signals $\Delta S(q,\tau)$, $\Delta S[r,\tau]$ can be calculated. These expressions represent exact second-order perturbation theory results.

3. 4. Visualizing Atomic Motions During Iodine Recombination

A great number of beautiful experiments have been realized using time-resolved x-ray diffraction or absorption techniques. Here we shall illustrate them on one example, showing how pump-probe x-ray techniques can be used to film atomic motions during recombination of photo dissociated iodine in solution. This reaction has been studied extensively in the past by laser spectroscopy and quantum chemistry.[21] A fair understanding of the underlying processes resulted from these studies. However, a fascinating challenge remained which is to film atomic motions during the reaction. This was realized as follows:[22]

In our experiment a I_2/CCl_4 solution was pumped by a 520 nm laser pulse, promoting the iodine molecule from its ground electronic state X to the excited states A, A', B and $^1\pi_u$ (Fig. 7). The laser excited I_2 dissociates rapidly into an unstable intermediate $(I_2)^*$. The latter decomposes, and the two iodine atoms recombine either geminately (a) or nongeminately (b):

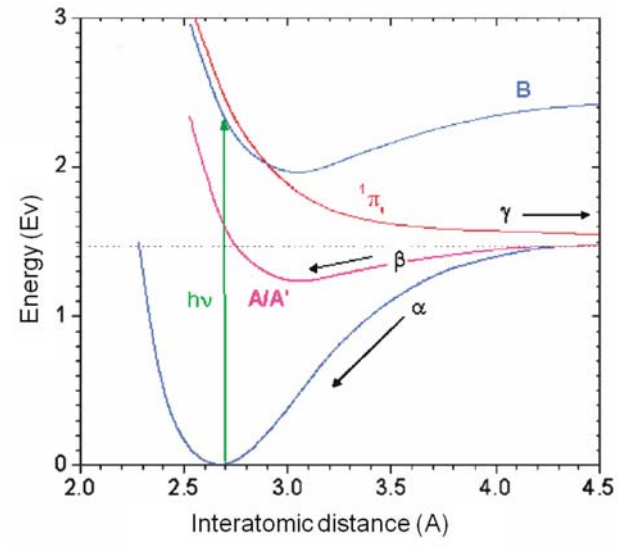

Fig. 7. Low lying electronic energy surfaces of I_2: the states X, A/A', and B are attractive, whereas the state $^1\pi_u$ is repulsive. The processes α, β and γ denote vibrational cooling along the X potential, geminate recombination through the states A, A', and nongeminate recombination, respectively.

$$I_2 + h\nu \rightarrow (I_2)^*,\ (I_2)^* \rightarrow I_2\,(a),\ (I_2)^* \rightarrow 2I \rightarrow I_2\,(b)$$

Atomic motions involved in this reaction were probed by x-ray pulses for a number of time delays τ. The duration of x-ray pulses was 100 ps. A collection of diffraction patterns were then transformed into a series of real-space snapshots by Fourier sine transforming the experimental signals. When the sequence of snapshots was joined together, it formed a film of the atomic motions during recombination. As the times considered in these experiments were long compared to the duration of the x-ray pulse, no deconvolution was necessary.

The detailed description of the observed signals is as follows. The first minimum in $\Delta S[r,\tau]$ at 2.7 Å at early times is due to the depletion of the X state molecular iodine from the laser excitation (Fig.8). The excited molecules then reach the excited electronic states A, A', B and $^1\pi_u$, and a maximum appears around 3.2 Å. Moreover, the energy transfer induces a rearrangement of the structure of the liquid, initially without any observable thermal expansion. New minima in $\Delta S[r,\tau]$, appear at 4.0 and 6.2 Å. Molecular dynamics simulations assigned them to changes in the intermolecular Cl-Cl distances in liquid CCl_4. At later times, the excited molecules all relax, and thermal expan-

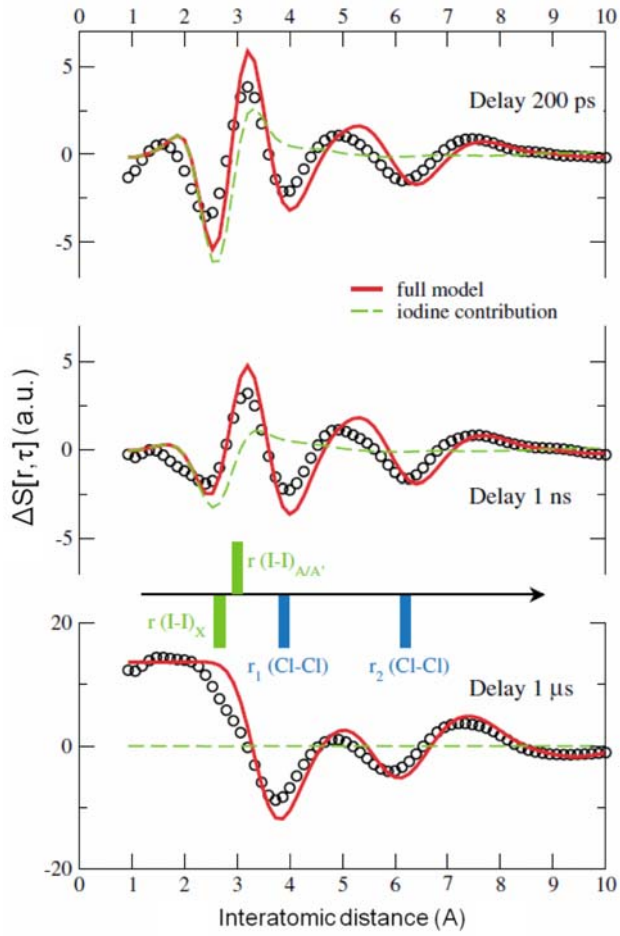

Fig. 8. Change in the atom-atom pair distribution function $g_{I-I}(r,\tau)$ for τ = 200 ps, 1 ns and 1μs. The green bars indicate the bond lengths of iodine in the states X and A/A'. The blue bars show the positions of the first two intermolecular peaks in the distribution function $g_{Cl-Cl}(r)$. These chlorine atoms are located in the first solvation shell of CCl_4.

sion is completed. The strong increase in $\Delta S[r,\tau]$ observed at small r's is due to the decrease of the mass density ρ_M of CCl_4. In turn, the features observed at large r's reflect the variations in the intermolecular Cl-Cl distances due to thermal expansion. Filming of atomic motions in liquids was thus accomplished. There is one reason for regret, however. As the x-ray pulse duration was of the order of 100 ps, and as no deconvolution was realized, the final bond reformation of nascent iodine molecules was not detected.

3. 5. Complementary Information

This Section can be concluded providing some additional information to the readers who may wish to go deeper into this field. In fact, a number of experiments have been realized using time-resolved x-ray techniques, both in diffraction and in absorption. As far as diffraction is concerned, one can cite interesting papers concerning the structure of short lived chemical species.[23–26] Another important direction of investigation refers to biological systems and their temporal evolution. Time-resolved crystallography was employed to explore how a protein functions,[27] whereas time-resolved wide-angle x-ray diffraction was applied to study structural dynamics of proteins in solution.[28] The behavior of laser excited nanoparticles dissolved in water has also been studied with much care.[29] In addition to time-resolved diffraction experiments, several time-resolved absorption experiments merit to be mentioned. They concern organometallic molecules like ruthenium (II) tris-2, 2'-bipiridine,[30] or they refer to the light-induced spin crossover dynamics in an iron (II) complex.[31] And – the last but not the least – there is much hope that with ultrafast XFEL x-ray sources new quantum phenomena will be discovered. A preliminary work is already going on in this direction.[32]

4. Conclusions

Ultrafast optical and x-ray techniques permit to visualize atomic motions during chemical reactions in real time. Picosecond as well as sub-picosecond time scales became accessible to experimental scrutiny. These methods provide a direct insight into the most intimate chemical processes such as birth of a new molecule, modification of their structure upon optical excitation, etc. The same techniques are also employed successfully in molecular biology and permit between other to explore motions of protein chains. Will this run to short times be stopped at femtosecond time scales? Probably not, the most recent attempts tend to explore attosecond time scales. Where is the end of this course?

5. References

1. Y. R Shen, The Principles of Nonlinear Optics (John Wiley & Sons, New York, 1984).
2. S. Mukamel, Principles of Nonlinear Optical Spectroscopy (Oxford University Press, New York, 1999).
3. M. Cho, Two-Dimensional Optical Spectroscopy (CRC Press, 2009).
4. Ch. Bressler and M. Chergui, *Journal* **2004,** *104,* 1781.
5. S. Bratos and M. Wulff, *Advances in Chemical Physics* **2008,** *317,* 1.
6. M. Chergui and A. H. Zewail, *Chem. Phys. Chem.* **2009,** *10,* 28.
7. S. Bratos and J-Cl. Leicknam*, J. Chem. Phys.* **1994,** *101,* 4536.
8. G. Gale, G. Gallot, F. Hache, N. Lascoux, S. Bratos and J-Cl. Leicknam, *Phys. Rev. Lett.* **1999,** *82,* 1068.
9. A. Novak, *Struct. Bonding* **1974,** *18,* 177.
10. S. Bratos, J-Cl. Leicknam and S. Pommeret, *J. Mol. Struct.* **2010,** *976,* 270.
11. H. Graener, G. Seifert and A. Laubereau, *Phys. Rev. Lett.* **1991,** *66,* 2092.
12. S. Woutersen, U. Emmerichs, H-K. Nieuhuys and H. Bakker, *Phys. Rev. Lett.* **1998,** *81,* 1106.
13. J. Stenger, D. Madsen, P. Hamm, E. Nibbering and T. Elssaeser, *Phys. Rev. Lett.* **2001,** *87,* 027401.
14. R. Rey, K. B. Moeller and J. T. Hynes, *J. Phys. Chem.* **2002,** *A 106,* 11993.
15. C. J. Fecko, J. D. Eaves, J. J. Loparo, A. Tokmakoff and P. I. Geissler*, Science* **2003,** *301,* 1698.
16. S. Yeremenko, M. S. Pshenichnikov and D. A. Wiersma*, Chem. Phys. Lett.* **2003,** *369,* 107.
17. J. R. Schmidt, S. A. Corcelli and J. L. Skinner*, J. Chem. Phys.* **2005,** *123,* 044513.
18. H. Iglev, M. Schmeisser, H. Simeonidis, A. Thaller and A. Laubereau, *Nature* **2006,** *439,* 183.
19. S.M. Ben-Nun, Jianshu Cao and K. Wilson, *J. Phys. Chem.* **1997,** *A 101,* 8743.
20. S. Bratos, F. Mirloup, R. Vuilleumier and M. Wulff, *J. Chem. Phys.* **2002,** *116,* 10615.
21. A. L. Harris, J. K. Brown and C. B. Harris, Annu. *Rev. Phys. Chem.* **1988,** *39,* 341.
22. A. Plech, M. Wulff, S. Bratos, F. Mirloup, R. Vuilleumier, F. Schotte and Ph. A. Anfinrud, *Phys. Rev. Lett*. **2004,** *92,* 125505.
23. R. Neutze, R. Wouts, S. Techert, J. Davidson, M. Kocsis, A. Kirrander, F. Schotte and M. Wulff, *Phys. Rev. Lett*. **2001,** *87,* 195508.
24. H. Ihee, M. Lorenc, T. K. Kim, Q. Y. Kong, M. Cammarata, J. H Lee, S. Bratos and M. Wulff, *Science* **2005,** *309,* 1223.
25. M. Cammarata, M. Lorenc, T. K. Kim, J. H. Lee, Q. Kong, E. Pontecorvo, E. Lo Russo, G. Schiro, A. Cupane, M. Wulff and H. Ihee, *J. Chem. Phys*. **2006,** *124,* 124504.
26. Q. Kong, J. H. Lee, M. Lo Russo, T. K. Kim, M. Lorenc, M. Cammarata, S. Bratos, T. Buslaps, V. Honkimaki, H. Ihee and M. Wulff, *Acta Crystal.* ***2010,*** *A66, 252.*

27. F. Schotte, M. Lim, T. A. Jackson, A. V. Smirnov, J. Soman, J. Olson, J. N. Phillips, M. Wulff and P. A. Anfinrud, *Science,* **2003,** *300,* 1944.
28. M. Cammarata, M. Levantino, F. Schotte, P. A. Anfinrud, F. Ewald, J. Choi, A. Cupane, M. Wulff and H. Ihee, *Nature Methods*, **2008,** ***5****,* 881.
29. A. Plech, V. Kotaidis, M. Lorenc and J. Boneberg, *Nature Phys*. **2006,** *2,* 44.
30. M. Saes, Ch. Bressler, R. Abela, D. Grolimund, S. L. Johnson, P. A. Heimann and M. Chergui, *Phys. Rev. Lett*. **2003,** *90,* 047403.
31. Ch. Bressler, C. Milne, V. T. Pham, A. Einahhas, R. M. Van der Veen, W. Gawelda, S. Johnson, P. Beaud, D. Grolimund, M. Kaiser,C. N. Borca, G. Ingold, R. Abela and M. Chergui, *Science* **2009,** *323,* 489.
32. A. Debnarova, S. Techert, S. Schmatz, *J. Chem. Phys*. **2011,** *134,* 054302.

Povzetek

Opisali smo metode ultrahitre optične spektroskopije in rentgenske difrakcije s časovno resolucijo. Predstavili smo eksperimentalne metode in teoretske pristope za interpretacijo eksperimentalnih rezultatov.
Uporabnost ultrahitrih tehnik smo pakazali na nekaj primerih. Snemanje atomskega gibanja med kemijsko reakcijo je eden od primerov uporabe. Kritično smo primerjali obe komplementarni tehniki. Vključene reference so v pomoč bralcu. Članek zaključujemo s pogledom v prihodnjost ultrahitre spektroskopije.